www.oeaw.ac.at

Johann Radon Institute for
Computational and Applied Mathematics
Austrian Academy of Sciences (ÖAW)

Extraction of the index of refraction by embedding multiple and close small inclusions

A. Alsaedi, F. Alzahrani, D. P. Challa, M. Kirane, M. Sini

RICAM-Report 2015-29

www.ricam.oeaw.ac.at

Extraction of the index of refraction by embedding multiple small inclusions

Ahmed Alsaedi [*] Faris Alzahrani[*] Durga Prasad Challa [†]
Mokhtar Kirane[*‡] Mourad Sini[§¶]

September 14, 2015

Abstract

We deal with the problem of reconstructing material coefficients from the far-fields they generate. By embedding small (single) inclusions to these media, located at points z in the support of these materials, and measuring the far-fields generated by these deformations we can extract the values of the total field generated by these media at the points z. The second step is to extract the values of the material coefficients from these internal values of the total field. The main difficulty in using internal fields is the treatment of their possible zeros.

In this work, we propose to deform the medium using multiple and close inclusions instead of only single ones. By doing so, we derive from the asymptotic expansions of the far-fields the internal values of the Green function, in addition to the internal values of the total fields. This is possible because of the deformation of the medium with multiple inclusions which generates scattered fields due to the multiple scattering between these inclusions. Then, the values of the index of refraction can be extracted from the singularities of the Green function. Hence, we overcome the difficulties arising from the zeros of the internal fields.

We test these arguments for the acoustic scattering by a refractive index in presence of inclusions modeled by the impedance type small obstacles. The reconstruction scheme is valid for arbitrary distributed multiple small inclusions. However, the error in the reconstruction is proportional to the distance between the pairs of inclusions, in addition to the radius of the small inclusions. An estimate of this error is provided. This estimate can be useful to find a reasonable balance between the desired accuracy of the reconstruction and the permissible closeness of the small inclusions (i.e. the small perturbations created by focusing waves for instance).

[*]Nonlinear Analysis and Applied Mathematics Research Group (NAAM), Department of Mathematics, Faculty of Sciences, King Abdulaziz University, P.O. Box 80203, Jeddah 21589, Saudi Arabia.

[†]Department of mathematics, Tallinn University of Technology, Tallinn 19068, Estonia. (Email: durga.challa@ttu.ee).

[‡]Laboratoire de Mathématiques, Pôle Sciences et Technologies, Université de La Rochelle, Avenue Michel Crépeau 17042, La Rochelle Cedex, France, (Email: mokhtar.kirane@univ-lr.fr).

[§]Corresponding author: Mourad Sini.

[¶]RICAM, Austrian Academy of Sciences, Altenbergerstrasse 69, A-4040, Linz, Austria. (Email: mourad.sini@oeaw.ac.at).

Keywords: Inverse acoustic scattering, small inclusions, multiple scattering, refraction index.

1 Introduction and statement of the results

1.1 Motivation of the problem

Let n be a bounded and measurable function in $\mathbb{R}^3$ such that the support of $(n-1)$ is a bounded domain Ω. We are concerned with the acoustic scattering problem

$$(\Delta + \kappa^2 n^2(x))V_n^t = 0 \text{ in } \mathbb{R}^3, \tag{1.1}$$

where $V_n^t := V_n^s + V^i$ and V^i is an incident field satisfying $(\Delta + \kappa^2)V^i = 0$ in $\mathbb{R}^3$. For simplicity, we take incident plane waves $V^i(x,\theta) := e^{i\kappa x\cdot\theta}$ where $\theta \in \mathbb{S}^2$ and $\mathbb{S}^2$ is the unit sphere. The scattered field V_n^s satisfies the Sommerfeld radiation condition:

$$\frac{\partial V_n^s}{\partial |x|} - i\kappa V_n^s = o\left(\frac{1}{|x|}\right), |x| \to \infty. \tag{1.2}$$

The scattering problem (1.1-1.2) is well posed, see [15]. Applying Green's formula to V_n^s, we can show that the scattered field $V_n^s(x,\theta)$ has the following asymptotic expansion:

$$V_n^s(x,\theta) = \frac{e^{i\kappa|x|}}{4\pi|x|}V_n^\infty(\hat{x},\theta) + O(|x|^{-2}), \quad |x| \to \infty, \tag{1.3}$$

where the function $V_n^\infty(\hat{x},\theta)$ for $(\hat{x},\theta) \in \mathbb{S}^2 \times \mathbb{S}^2$ is the corresponding far-field pattern.

Our interest in this work is related to the classical inverse scattering problem which consists of reconstructing $n(x)$, $x \in \Omega$, from the far-field data $V_n^\infty(\hat{x},\theta)$ for some $(\hat{x},\theta) \in \mathbb{S}^2 \times \mathbb{S}^2$. This type of problem is well studied and there are several algorithms to solve it in the case when $\hat{x}$ and θ are taken in the whole $\mathbb{S}^2$, see [25, 26, 27]. It is also known that this problem is very unstable. Precisely, the modulus of continuity is in general of logarithmic type, see [28].

Recently, based on a new type of experiments, a different approach was proposed, see for instance [3, 5] and the references therein. It is divided into two steps. In the first one, we deform the acoustic medium by small inclusions located in the region containing the support of $(n-1)$, and measure the far-fields generated by these deformations. From these far-fields, we can extract the total fields due to the medium n in the interior of the support of $(n-1)$. In the second step, we reconstruct $n(x)$ from these interior values of the total fields. Recently, there was an increase of interest in reconstructing media from internal measurements. This is also related to the hybrid methods introduced in the medical imaging community, see [4, 7, 8, 16, 17, 20] for different setups and models. In contrast to the instability of the classical inverse scattering problem, the reconstruction from internal measurements is stable, see [1, 6, 18, 29]. However, the disadvantage with internal fields, i.e. internal values of the total fields, is the existence of their zeros which need to be properly dealt with to stabilize any algorithm. To overcome this short coming, one can think of using measurements related to multiple frequencies $\kappa_1, \kappa_2, etc.$, see [2].

Our objective in this paper is to propose an alternative to overcome the last disadvantage. For this, we propose to deform the medium using multiple and close inclusions instead of just single inclusions. Then, measuring the generated far-fields by these multiple inclusions, we can extract, not only the internal total fields, but also the internal values of the Green's function related to the non deformed medium n. This is possible because by deforming the medium with multiple and close inclusions we generate scattered fields due to the multiple scattering between these inclusions. Precisely, the far-fields we measure encode at least the second order term in the Foldy-Lax approximation and not only the first order (or the Born approximation) as it is done when deforming with single or multiple but well separated inclusions. Finally, we extract the values $n(x)$, x in Ω, from the singularities of this Green's function. Hence, we avoid the problems coming from the zeros of the internal total fields.

The accuracy of the reconstruction is related to the minimum distance d between the pairs of inclusions, in addition to the radius of the perturbations a. In practice, the perturbations are created using focusing waves, see [4, 20] for instance, hence we are limited by the size related to the resolution of the used waves (acoustic waves for instance). In other words, the small perturbations cannot be very close. In our analysis, the ratio $\frac{a}{d}$ is of the form a^{1-t}, with a parameter $t \in [0, 1]$, and it can be chosen small by taking t near 0. This allows to have the minimum distance between the inclusions quite large compared to their sizes. Since the accuracy of the reconstruction, see Theorem 1.2, is of the order a^t, with t in $[0, t^*]$ with some $t^* < 1$, then one should find a reasonable balance between the limited resolution of the focusing waves, to be used to perturb the medium, and the desired accuracy of the reconstruction. More details related to this issue are provided in Remark 1.3.

1.2 Deformation by multiple inclusions

We give the details of this approach by using inclusions of the form of obstacles of impedance type. Let B be the ball with the center at the origin and radius 1. We set $D_m := aB + z_m$ to be the small bodies characterized by the parameter $a > 0$ and the locations $z_m \in \mathbb{R}^3$, $m = 1, \dots, M$. We denote by U^s the acoustic field scattered by the M small bodies $D_m \subset \mathbb{R}^3$, due to the incident field U^i (mainly the plane incident waves $U^i(x, \theta) := V^i(x, \theta) := e^{ikx\cdot\theta}$ with the incident direction $\theta \in \mathbb{S}^2$, where $\mathbb{S}^2$ being the unit sphere), with impedance boundary conditions. Hence the total field $U^t := U^i + U^s$ satisfies the following exterior impedance problem for the acoustic waves

$$(\Delta + \kappa^2 n^2(x))U^t = 0 \text{ in } \mathbb{R}^3 \setminus \left(\overset{M}{\underset{m=1}{\cup}} \bar{D}_m \right), \tag{1.4}$$

$$\left. \frac{\partial U^t}{\partial \nu_m} + \lambda_m U^t \right|_{\partial D_m} = 0, \; 1 \leq m \leq M, \tag{1.5}$$

$$\frac{\partial U^s}{\partial |x|} - i\kappa U^s = o\left(\frac{1}{|x|}\right), \; |x| \to \infty. \tag{1.6}$$

The scattering problem (1.4)-(1.6) is well posed, see [14, 15], and we can also allow $\Im \lambda_m$ to be negative, see [13].

Definition 1.1. *We define*

1. $d := \min\limits_{\substack{m \neq j \\ 1 \leq m,j \leq M}} d_{mj}$, *where* $d_{mj} := dist(D_m, D_j)$.

2. $\kappa_{\max}$ *as the upper bound of the used wave numbers, i.e.* $\kappa \in [0, \kappa_{\max}]$.

   The distribution of the scatterers is modeled as follows:

3. *the number* $M := M(a) := O(a^{-s}) \leq M_{max} a^{-s}$ *with a given positive constant* M_{max}.

4. *the minimum distance* $d := d(a) \approx a^t$, *i.e.* $d_{min} a^t \leq d(a) \leq d_{max} a^t$, *with given positive constants* d_{min} *and* d_{max}.

5. *the surface impedance* $\lambda_m := \lambda_{m,0} a^{-\beta}$, *where* $\lambda_{m,0} \neq 0$ *and might be a complex number.*

Here the real numbers s, t and β are assumed to be non negative. We call $M_{max}, d_{min}, d_{max}$ and κ_{max} the set of the a priori bounds. In ([13], Corollary 1.3), we have shown that there exist positive constants a_0, λ_-, λ_+ [1] depending only on the set of the a priori bounds and on $n_{max} := \|n\|_{L^\infty(\Omega)}$ such that if

$$a \leq a_0,\ |\lambda_{m,0}| \leq \lambda_+,\ |\Re(\lambda_{m,0})| \geq \lambda_-, \quad \beta \leq 1, \quad s \leq 2 - \beta, \quad \frac{s}{3} \leq t, \tag{1.7}$$

then the far-field pattern $U_n^\infty(\hat{x}, \theta)$ has the following asymptotic expansion

$$U_n^\infty(\hat{x}, \theta) = V_n^\infty(\hat{x}, \theta) + \sum_{m=1}^{M} V_n^t(z_m, -\hat{x}) \mathbb{Q}_m + O\left(M\, \mathcal{C}\, a\right), \tag{1.8}$$

uniformly in $\hat{x}$ and θ in $\mathbb{S}^2$. Here $\mathcal{C} := \max_m C_m$. The constant appearing in the estimate $O(.)$ depends only on the set of the a priori bounds, λ_-, λ_+ and on n_{max}. The coefficients $\mathbb{Q}_m$, $m = 1, ..., M$, are the solutions of the following linear algebraic system

$$\mathbb{Q}_m + \sum_{\substack{j=1 \\ j \neq m}}^{M} C_m G_\kappa(z_m, z_j) \mathbb{Q}_j = -C_m V^t(z_m, \theta), \tag{1.9}$$

for $m = 1, ..., M$, where

$$C_m := \frac{\lambda_m |\partial D_m|}{-1 + \lambda_m I_m} \tag{1.10}$$

and $G_\kappa(\cdot, \cdot)$ is the Green function corresponding to the scattering problem (1.4)-(1.6).

The quantity $I_m := \int_{\partial D_m} \Phi_0(s_m, t) ds_m, t \in \partial D_m$, is a constant if D_m is a ball and this constant is equal to the radius of D_m, i.e. $I_m = a$. The algebraic system (1.9) is invertible under the condition:

$$s \leq 2 - \beta. \tag{1.11}$$

[1] In the case where $s < 2 - \beta$, we need no a priori conditions on λ_-, λ_+.

We use surface impedance functions of the form $\lambda_m = \lambda_{0,m} a^{-\beta}$, i.e. with $\lambda_{0,m} \neq 1$ in the case $\beta = 1$, so that the constants

$$C_m = \frac{4\pi \, a^{2-\beta} \, \lambda_{0,m}}{-1 + \lambda_{0,m} a^{1-\beta}} \tag{1.12}$$

are well defined. In the subsequent sections, we choose $\beta = 1$ and $\lambda_{0,m} := 1 - a^h$, $h \geq 0$. In this case

$$C_m = -4\pi a^{1-h}(1 - a^h). \tag{1.13}$$

Hence (1.8) becomes

$$U_n^\infty(\hat{x}, \theta) = V_n^\infty(\hat{x}, \theta) + \sum_{m=1}^{M} V_n^t(z_m, -\hat{x}) \mathbb{Q}_m + O\left(a^{2-s-h}\right), \tag{1.14}$$

uniformly in $\hat{x}$ and θ in $\mathbb{S}^2$.

1.3 The extraction formulas

We proceed in three steps in collecting the measured data:

1. First step. We measure the far-fields before making any deformation. In this case the collected data are $V_n^\infty(\theta_i, \theta_j)$, $i, j =$ ..., $N_0 \geq 2M$ including at least one backscattering measurement $V_n^\infty(-\theta_{i_0}, \theta_{i_0})$.

2. Second step. We deform the medium by single inclusions $z_i^l, i = 1, ..., M$, $l = 1, 2$, and then measure the corresponding data $U_n^\infty(z_i^l, -\theta_j, \theta_j)$, for the directions θ_j, $j = 1, ..., N_0$ and $i = 1, 2, ..., M$, $l = 1, 2$, keeping in mind that we redo the experiment by moving the inclusion centered at z_i^l for $i = 1, 2, ..., M$ and $l = 1, 2$, see Fig 1.

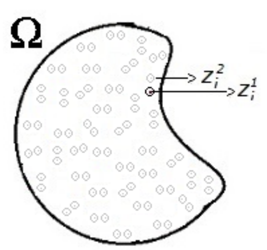

Figure 1: The figure describes the experiments in step 2. We create only one inclusion and measure the corresponding far-fields. Then, we move the inclusion inside Ω.

3. Third step. We deform the medium using two inclusions close to each other, or a set of $2M$ inclusions two-by-two close to each other, i.e. every couple of two points z_i^1 and z_i^2, $i = 1, ..., M$, in Ω, are such that $|z_i^2 - z_i^1| \sim a^t$, as $a \to 0$, with $t > 0$, see Fig 2. In this case, the collected data are $W_n^\infty(\theta_i, \theta_j)$, $i, j = 1, ..., N_0 \geq 2M$. Compared to step 2, here we can use all the inclusions at once.

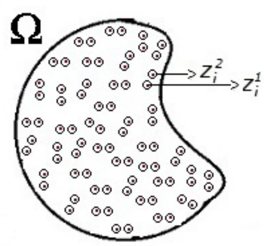

Figure 2: The figure describes the experiments in step 3. We create multiple ($2M$) inclusions distributed two by two close to each other and then we measure the corresponding far-fields.

The reconstruction formulas of the index of refraction from the described measured data are summarized in the following theorem.

Theorem 1.2. *Assume n to be a measurable and bounded function in $\mathbb{R}^3$ such that the support of $(n-1)$ is a bounded domain Ω. Let the non negative parameters β, s, h and t describing the set of the small inclusions, embedded in Ω, be such that*

$$\beta = 1, \; s < h \;\; \text{and} \;\; h + 2t < 1. \tag{1.15}$$

We have the following formulas:

1. *The total field $V_n^t(z_j^l, \theta_j)$ can be recovered from $U_n^\infty(z_i^l, \, -\theta_j, \theta_j) - V_n^\infty(-\theta_j, \theta_j)$ as follows:*

$$C_{i,l}^{-1}\left[U_n^\infty(z_i^l, -\theta_j, \theta_j) - V_n^\infty(-\theta_j, \theta_j)\right] = -[V_n^t(z_i^l, \theta_j)]^2 + O(a), \tag{1.16}$$

   for $j = 1, 2, ..., N_0$; $\;l = 1, 2$ and $i = 1, 2, ..., M$. Here $C_{i,l}$ is the capacitance of the small inclusion centered at the point z_i^l.

2. *Knowing the total fields $V_n^t(z_i^l, \theta_j), l = 1, 2$ and $i = 1, 2, ..., M$ and $j = 1, 2, ..., N_0, \;\; N_0 \geq 2M$, the values of the Green function $G_\kappa(z_i^1, z_i^2), i = 1, 2, ..., M$ can be recovered as follows. We have*

$$G_\kappa(z_i^1, z_i^2) := (\tilde{\boldsymbol{G}}_\kappa)_{2i-1,2i} \;, \; \text{for } i = 1, 2, ..., M \tag{1.17}$$

   where the matrix $\tilde{\boldsymbol{G}}_\kappa$ is computable as

$$(\boldsymbol{V}\boldsymbol{V}^\top)^{-1}\boldsymbol{C}^{-2}\,\boldsymbol{V}[\mathbf{W}_n^\infty - \mathbf{V}_n^\infty]\,\boldsymbol{V}^\top(\boldsymbol{V}\boldsymbol{V}^\top)^{-1} - \boldsymbol{C}^{-1} = \tilde{\boldsymbol{G}}_\kappa + \;\; O\left(a^{1-h-2t} + a^{h-s}\right) \tag{1.18}$$

   with the matrix $\boldsymbol{V}$ constructed from (1.16) via $(\boldsymbol{V})_{i,j} := V_n^t(z_i^l, \theta_j)$, $l = 1, 2, i = 1, .2, ..., M$ and $j = 1, 2, ..., N_0$ and $\boldsymbol{C} := \operatorname{diag}\{C_{i,l}\}$. [2] *The matrices $\mathbf{W}_n^\infty$ and $\mathbf{V}_n^\infty$ are defined as $(\mathbf{W}_n^\infty)_{i,j} := W_n^\infty(\theta_i, \theta_j)$ and $(\mathbf{V}_n^\infty)_{i,j} := V_n^\infty(\theta_i, \theta_j)$, $i = 1, ..., 2M$ and $j = 1, ..., N_0$.*

[2]The matrix $\operatorname{diag}\{C_{i,l}\}$ is diagonal and the diagonal values are defined by the vector $\{C_{1,1}, C_{1,2}, C_{2,1}, C_{2,2}, ..., C_{M,1}, C_{M,2}\}$. Since the capacitances are equal $C_{i,l} = -4\pi a^{1-h}(1-a^h)$ as the inclusions are the same, i.e. balls of radius a, we have $\operatorname{diag}\{C_{i,l}\} = -4\pi a^{1-h}(1-a^h)I_{3M}$ where I_{3M} is the identity matrix in $\mathbb{R}^{3M}$.

3. *If, in addition, n is of class C^α, $\alpha \in (0,1]$, then*[3] *from the values of the Green function $G_n(z_i^1, z_i^2), i = 1, 2, ..., M$, we reconstruct the values of the index of refraction $n(z_i^l)$, $i = 1, 2, ..., M$, as follows:*

$$n(z_j^l) = \left[\frac{4\pi}{i\kappa} G_\kappa(z_j^2, z_j^1) - \frac{1}{i\kappa |z_j^2 - z_j^1|}\right] + O(a^t), \quad t > 0. \tag{1.19}$$

Remark 1.3. *We make the following observations:*

1. *We observe that due to the error $O(a^t)$, for $i = 1, .2, ..., M$, we do not distinguish between $n(z_i^1)$ and $n(z_i^2)$ since $|z_i^1 - z_i^2| \sim a^t$, as $a \to 0$ and hence $|n(z_i^1) - n(z_i^2)| = O(a^t)$ (in the best case $\alpha = 1$). Hence these formulas provide the values of $n(z_i)$, for $i = 1, .2, ..., M$, where $z_i := z_i^l$ for either $l = 1$ or $l = 2$.*

2. *We can take $s = 0$, which means that the number M of the small inclusions is moderate, i.e. it is not growing when $a \to 0$. In this case t lies in $[0, t^*]$ where t^*, which depends on h, is given by the combination of the formulas (1.16), (1.18) and (1.19). Hence the ratio between the radius a and the minimum distance $d \approx a^t$ is of the order $\frac{a}{d} \approx a^{1-t} << 1$ as $a << 1$. This rate becomes significantly smaller when t approaches 0. This means that the small perturbations do not need to be very close to apply the reconstruction formulas in Theorem 1.2. This makes sense and can be useful in practice since, due to the resolution limit, it is delicate to use focusing waves to create close small deformations. The price to pay is that we will have less accuracy in the reconstruction, see the formula (1.19) for instance. Hence, one needs to find a compromise between the desired accuracy of the reconstruction and the permissible closeness of the small perturbations created by focusing waves.*

3. *The importance of the parameter t, describing the closeness of the small inclusions, appears only in the last step (i.e. the point 3. in Theorem 1.2) to compute the values of n using the singularity analysis of G. If we need to choose t very small, then we can also use other methods to compute $n(x)$ from $G(x, z)$. For instance, from the Lippmann-Schwinger equation $G(x, z) = \Phi(x, z) + \kappa^2 \int_\Omega (n^2 - 1)(t) G(t, z) \Phi(t, x) dt$, $x, z \in \Omega$, we can compute $(n^2 - 1)(x) G(x, z)$ by inverting an integral equation of the first kind having as a kernel $\Phi(x, z)$. Knowing $G(x, z)$ and $(n^2 - 1)(x) G(x, z)$ for a sample of points $x, z \in \Omega$, we can reconstruct n from the formula $(n^2 - 1)(x) = \frac{(n^2-1)(x)G(x,z)}{G(x,z)}$. The denominator $G(\cdot, z)$ is not vanishing if we choose appropriately different values of the source points z in Ω.*

[3] We can also take $\alpha = 0$, i.e. n is only continuous, and obtain (1.19) with an appropriate change in the error term.

2 Proof of Theorem 1.2

2.1 Step 1: use of single inclusion to extract the field $V_n^t(z_i^l, \theta_j),\ z_i^l \in \Omega$

We create one single inclusion located at a selected point z_i^l in Ω. This means that we take $M = 1$ in the asymptotic expansion (1.8), i.e. $U_n^\infty(z_i^l, \hat{x}, \theta) - V_n^\infty(\hat{x}, \theta) = V_n^t(z_i^l, -\hat{x})\mathbb{Q} + O\left(a^{2-h}\right)$ and $\mathbb{Q} = -C_{i,l}V_n^t(z_i^l, \theta)$. Hence

$$U_n^\infty(z_i^l, \hat{x}, \theta) - V_n^\infty(\hat{x}, \theta) = -C_{i,l}V_n^t(z_i^l, -\hat{x})V_n^t(z_i^l, \theta) + \ O\left(a^{2-h}\right). \tag{2.1}$$

From the backscattered data $U_n^\infty(z_i^l, -\theta_j, \theta_j)$, we obtain the total field $V_n^t(z_i^l, \theta_j)$ at the point z_i^l since $C_{i,l} := -4\pi a^{1-h}(1-a^h)$ is known. Indeed, from (2.1) we derive the formula

$$C_{i,l}^{-1}\left[U_n^\infty(z_i^l, -\theta_j, \theta_j) - V_n^\infty(-\theta_j, \theta_j)\right] = -(V_n^t(z_i^l, \theta_j))^2 + \ O\left(a\right). \tag{2.2}$$

2.2 Step 2: Use of multiple inclusions to extract the Green's function $G_\kappa(x, z),\ x, z \in \Omega$

In this case, we create multiple inclusions located two by two close to each other, i.e. every couple of two points z_i^1 and z_i^2, $i = 1, ..., M$, in Ω, are such that $|z_i^2 - z_i^1| \sim a^t$, as $a \to 0$, with $t > 0$. We use the number M of the small inclusions to be dense enough in Ω, i.e. $M = O(a^{-s})$ with $s < 1$. For convenience, we use the notation C_m's instead of $C_{i,l}$'s by adopting the ordering $C_1 := C_{1,1}, C_2 := C_{1,2}, C_3 := C_{2,1}, C_4 := C_{2,2}$,..., etc.

From the asymptotic expansion (1.8), we have

$$W_n^\infty(\hat{x}, \theta) - V_n^\infty(\hat{x}, \theta) = \sum_{m=1}^{2M} V_n^t(z_m, -\hat{x})\mathbb{Q}_m + O\left(M\mathcal{C}a\right), \tag{2.3}$$

where

$$\mathbb{Q}_m + \sum_{\substack{j=1 \\ j\neq m}}^{2M} C_m G_\kappa(z_m, z_j)\mathbb{Q}_j \ \ = \ \ -C_m V^t(z_m, \theta), \tag{2.4}$$

for $m = 1, ..., 2M$. Hence, we rewrite (2.3) as

$$W_n^\infty(\hat{x}, \theta) - V_n^\infty(\hat{x}, \theta) = \mathbf{V}_n^\top(-\hat{x})\mathbf{B}^{-1}\mathbf{V}_n(\theta) + \ O\left(M\mathcal{C}a\right), \tag{2.5}$$

where we use the vector $\mathbf{V}_n(\theta) := \left[V_n^t(z_1, \theta), V_n^t(z_2, \theta), ..., V_n^t(z_{2M}, \theta)\right]^\top$ and the matrix $\mathbf{B}$ whose components are $\mathbf{B}_{i,j} := -G_\kappa(z_i, z_j)$ and $\mathbf{B}_{i,i} := -C_i^{-1}$ for $i = 1, 2, ..., 2M$.

We use a number N of directions of incidences (and hence of propagation directions) larger than the number of sampling points $z_i, 1, ..., 2M$, i.e. $2M$ directions, where we want to evaluate the index of refraction. With this number at hand, the matrix

$$\mathbf{V}_n := [\mathbf{V}_n(\theta_1), \mathbf{V}_n(\theta_2), ..., \mathbf{V}_n(\theta_N)] \tag{2.6}$$

has a full rank and hence $\mathbf{V}_n\mathbf{V}_n^\top$ is invertible. Precisely, we have the following lemma.

Lemma 2.1. *There exists $N_0 \in \mathbb{N}$ such that if the number N of incident directions θ_j, $j = 1, ..., N$ is larger than N_0, i.e. $N \geq N_0$ then the vectors $\mathbf{V}_n^t(\theta_j) := [V_n^t(z_1, \theta_j), V_n^t(z_2, \theta_j), ..., V_n^t(z_{2M}, \theta_j)]^\top$, $j = 1, ..., N$ are linearly independent.*

Proof. We observe, by the mixed reciprocity relations, that $V_n(z_i, \theta_j) = G_n^\infty(-\theta_j, z_i)$, where $G_n^\infty(-\theta_j, z_i)$ is the far-field in the direction $-\theta_j$ of the point source $G_n(x, z_j)$ supported at the source point z_i. We recall that the point source $G_n(x, z_j)$ is the Green function of the model (1.1). With this relation at hand, the proof of the lemma follows the same arguments in [19] where it is done for the vectors $(e^{-i\kappa\theta_j \cdot z_i})_{i=1}^{2M}$ and $j = 1, ..., N$, with N large enough. We omit the details. Observe that $V_n^t(z_i, \theta_j) = e^{i\kappa\theta_j \cdot z_i}$ if the index of refraction n is equal to unity in $\mathbb{R}^3$. □

Hence measuring the data $\mathbf{W}_n^\infty$ and $\mathbf{V}_n^\infty$ recalling that

$$(\mathbf{W}_n^\infty)_{i,j} := (W_n^\infty(-\theta_i, \theta_j)),\ i = 1, ..., 2M, \quad j = 1, ..., N_0 \tag{2.7}$$

and

$$(\mathbf{V}_n^\infty)_{i,j} := (V_n^\infty(-\theta_i, \theta_j)),\ i = 1, ..., 2M, \quad j = 1, ..., N_0, \tag{2.8}$$

we obtain the formula

$$\mathbf{W}_n^\infty - \mathbf{V}_n^\infty = \mathbf{V}^\top \mathbf{B}^{-1} \mathbf{V} \ + O\left(a^{2-s-h}\right). \tag{2.9}$$

Observe that $\mathbf{B}^{-1} = -\left(I + \mathbf{C}\tilde{\mathbf{G}}_\kappa\right)^{-1} \mathbf{C}$ where $\mathbf{C} := diag\,(C_i)$ and $\left(\tilde{\mathbf{G}}_\kappa\right)_{i,i} := 0, i = 1, 2, ..., 2M$ and $\left(\tilde{\mathbf{G}}_\kappa\right)_{i,j} := G_\kappa(z_i, z_j), i \neq j, i, j = 1, 2, ..., 2M$. Hence we can write

$$\mathbf{B}^{-1} = -\mathbf{C} + \mathbf{C}\tilde{\mathbf{G}}_\kappa \mathbf{C} + O(\max_i \{C_{z_i}\} \|\mathbf{C}\mathbf{G}_\kappa\|_2^2) \tag{2.10}$$

where $\|\|_2$ is the l_2-norm for matrices.

We recall that we choosed these points $z_i, i = 1, 2, ..., 2M$ appropriately so that they are two by two close to each other. Precisely, every couple of two points z_i^1 and z_i^2, $i = 1, ..., M$, in Ω, are such that $|z_i^2 - z_i^1| \sim a^t$ with $t \in (0, 1)$, as $a \to 0$. In addition, $\min_{i \neq j} |z_i^l - z_j^l| \geq d_0$, $l = 1, 2$, where $d_0 > 0$ is independent of a. With such a choice, we see that

$$\mathbf{B}^{-1} = -\mathbf{C} + \mathbf{C}\tilde{\mathbf{G}}_\kappa \mathbf{C} + O\left(a^{3-3h-2t}\right) \tag{2.11}$$

as $O(\max_i \{C_{z_i}\} \|\mathbf{C}\tilde{\mathbf{G}}_\kappa\|_2^2) = O(a^{3-3h-2t})$.

Finally, from the matrix $\mathbf{B}$ we derive the values of the Green function at the sampled points $z_i,\ i = 1, 2, ..., 2M$, in Ω:

$$G_\kappa(z_i^1, z_i^2),\ i = 1, 2, ..., M. \tag{2.12}$$

Indeed, combining (2.9) and (2.11), we deduce that

$$\mathbf{W}_n^\infty - \mathbf{V}_n^\infty = -\mathbf{V}^\top \mathbf{C}\mathbf{V} \ + \mathbf{V}^\top \mathbf{C}\tilde{\mathbf{G}}_\kappa \mathbf{C}\mathbf{V} \ + \ O\left(a^{3-3h-2t} + a^{2-s-h}\right) \tag{2.13}$$

where $\mathbf{V}^\top \mathbf{C}\mathbf{V} \sim a^{1-h}$ and $\mathbf{V}^\top \mathbf{C}\tilde{\mathbf{G}}_\kappa \mathbf{C}\mathbf{V} \sim a^{2-2h-t}$. The approximation (2.13) will make sense, i.e. the error term is dominated by $-\mathbf{V}^\top \mathbf{C}\mathbf{V} \ + \mathbf{V}^t op \mathbf{C}\tilde{\mathbf{G}}_\kappa \mathbf{C}\mathbf{V}$, if $3 - 3h - 2t > 2 - 2h - t$

and $2-s-h > 2-2h-t$, i.e. $s < t+h < 1$. In addition, $\mathbf{V}^\top\mathbf{C}\tilde{\mathbf{G}}_\kappa\mathbf{C}\mathbf{V} = O(\mathbf{V}^\top\mathbf{C}\mathbf{V})$ if $2-2h-t \geq 1-h$, i.e. $t+h \leq 1$. Hence the approximation (2.13) makes sense if $s < t+h < 1$. This last condition is satisfied since we assumed that $s < h$ and $h+2t < 1$.

From Step 1, we showed already how to extract the matrices $\mathbf{V}$, hence we can compute $\mathbf{W}_n^\infty - \mathbf{V}_n^\infty - \mathbf{V}\mathbf{C}\mathbf{V}$. Since the matrix $\mathbf{C}$ is diagonal, with non zero entries, and the matrix $\mathbf{V}\mathbf{V}^\top$ is invertible, as $\mathbf{V}$ is full rank matrix, then we can recover the matrix $\tilde{\mathbf{G}}_\kappa$ as

$$\mathbf{C}^{-1}(\mathbf{V}\mathbf{V}^\top)^{-1}\mathbf{V}\left[\mathbf{W}_n^\infty - \mathbf{V}_n^\infty\right]\mathbf{V}^\top(\mathbf{V}\mathbf{V}^\top)^{-1}\mathbf{C}^{-1}+\mathbf{C}^{-1} = \tilde{\mathbf{G}}_\kappa + \ O(a^{2h-2})\, O\left(a^{3-3h-2t} + a^{2-s-h}\right) \tag{2.14}$$

or

$$\mathbf{C}^{-1}(\mathbf{V}\mathbf{V}^\top)^{-1}\mathbf{V}\left[\mathbf{W}_n^\infty - \mathbf{V}_n^\infty\right]\mathbf{V}^\top(\mathbf{V}\mathbf{V}^\top)^{-1}\mathbf{C}^{-1}+\mathbf{C}^{-1} = \tilde{\mathbf{G}}_\kappa + \ \ O\left(a^{1-h-2t} + a^{h-s}\right). \tag{2.15}$$

We see that $a^{h-s} = o(\tilde{\mathbf{G}}_\kappa)$ if $h-s > -t$,i.e. $t+h > s$ and $a^{1-h-2t} = o(\tilde{\mathbf{G}}_\kappa)$ if $1-h-2t > -t$, i.e. $t+h < 1$. Hence (2.15) makes sense if $s < t+h < 1$. As mentioned above, this last condition is satisfied since we assumed that $s < h$ and $h+2t < 1$.

Finally, we set

$$G_\kappa(z_i^1, z_i^2) := (\tilde{\mathbf{G}}_\kappa)_{2i-1,2i}, \quad \text{for } i = 1, 2, ..., M \tag{2.16}$$

as the reconstructed values of the Green function G_κ at the sampling points (z_i^1, z_i^2), $i = 1, 2, ..., M$.

2.3 Step 3: Extraction of the index of refraction from the Green function

We start with the following lemma

Lemma 2.2. *We have the asymptotic expansion:*

$$G_\kappa(x, z_j) = \frac{e^{i\kappa n(z_j)|x-z_j|}}{4\pi|x-z_j|} + O(|x-z_j|), \quad \text{as } |x-z_j| \to 0. \tag{2.17}$$

Proof. We know that $(\Delta + \kappa^2 n^2(x))G_\kappa = -\delta$, in $\mathbb{R}^3$ and $\Phi_{\kappa,j}(x,z) := \frac{e^{i\kappa n(z_j)|x-z|}}{4\pi|x-z|}$ satisfies $(\Delta + \kappa^2 n^2(z_j))\Phi_\kappa = -\delta$, in $\mathbb{R}^3$, where both G_κ and $\Phi_{\kappa,j}$ satisfy the Sommerfeld radiation condition. Then $H_{\kappa,j}(x,z) := (G_\kappa - \Phi_{\kappa,j})(x,z)$ satisfies the same radiation condition and

$$(\Delta + \kappa^2 n^2(z_j))H_{\kappa,j} = \kappa^2(n^2(z_j) - n^2(x))G_\kappa, \text{ in } \mathbb{R}^3. \tag{2.18}$$

Multiplying both sides of (2.18) by $\Phi_{\kappa,j}$ and integrating over a bounded and smooth domain B we obtain:

$$\begin{aligned} H_{\kappa,j}(x,z) \ &= \ -\kappa^2 \int_B (n^2(z_j) - n^2(t))\Phi_{\kappa,j}(t,x)G_\kappa(t,z)dt \\ &\quad - \int_{\partial B} H_{\kappa,j}(t,z)\partial_{\nu(t)}\Phi_{\kappa,j}(t,x)ds(t) + \int_{\partial B} \partial_{\nu(t)}H_{\kappa,j}(t,z)\Phi_{\kappa,j}(t,x)ds(t), \end{aligned} \tag{2.19}$$

and then

$$
\begin{aligned}
\nabla_x H_{\kappa,j}(x,z_j) &= -\kappa^2 \int_B (n^2(z_j)-n^2(t))\Phi_{\kappa,j}(t,x)\nabla_x G_\kappa(t,z_j)dt \qquad (2.20)\\
&\quad - \int_{\partial B} H_{\kappa,j}(t,z_j)\nabla_x \partial_{\nu(t)}\Phi_{\kappa,j}(t,x)ds(t) + \int_{\partial B} \partial_{\nu(t)} H_{\kappa,j}(t,z_j)\nabla_x\Phi_{\kappa,j}(t,x)ds(t).
\end{aligned}
$$

Here, we choose B such that $\Omega \subset\subset B$. Since $(n^2(z_j)-n^2(t))\nabla G_\kappa(t,z_j) = O(|t-z_j|^{-2+\alpha}), t \in B$, as the singularity of $\nabla_x G_\kappa(t,-z_j)$ is of the order $|t-z_j|^{-2}$, and $n^2(z_j)-n^2(t) = O(|t-z_j|^{\alpha})$, since n is of class C^α, we deduce that $\int_B (n^2(z_j)-n^2(t))\Phi_{\kappa,j}(t,x)\nabla_x G_\kappa(t,z_j)dt = O(\int_B |t-z_j|^{-2+\alpha}|t-x|^{-1}dt) = O(1),\ x \in B$ since $\alpha > 0$, see ([30], Lemma 4.1), for instance, for the such integrals o f of singular functions. The two last integrals appearing in (2.20) are of the order $O(1)$ for $x \in \Omega \subset\subset B$.

Now, let $B_{z_j,r}$ be the ball of center z_j and radius r, $r << 1$. We use (2.19) applied to $B_{z_j,r}$ instead of B:

$$
\begin{aligned}
H_{\kappa,j}(x,z) &= -\kappa^2 \int_{B_{z_j,r}} (n^2(z_j)-n^2(t))\Phi_{\kappa,j}(t,x)G_\kappa(t,z)dt \qquad (2.21)\\
&\quad - \int_{\partial B_{z_j,r}} H_{\kappa,j}(t,z)\partial_{\nu(t)}\Phi_{\kappa,j}(t,x)ds(t) + \int_{\partial B_{z_j,r}} \partial_{\nu(t)} H_{\kappa,j}(t,z)\Phi_{\kappa,j}(t,x)ds(t)
\end{aligned}
$$

for $x \in B_{z_j,r}$. We see that

$$
\int_{B_{z_j,r}} (n^2(z_j)-n^2(t))\Phi_\kappa(t,x)G_\kappa(t,z_j)dt = O\Big(\int_{B_{z_j,r}} |t-z_j|^{-1+\alpha}|t-x|^{-1}ds(t)\Big),\ \text{for } x \in B_{z_j,r}
$$

which we can rewrite as

$$
\int_{B_{z_j,r}} (n^2(z_j)-n^2(t))\Phi_\kappa(t,x)G_\kappa(t,z_j)dt = O\Big((\int_{B_{z_j,r}} |t-z_j|^{-2+2\alpha}ds(t))^{\frac{1}{2}}(\int_{B_{x,2r}} |t-x|^{-2}ds(t))^{\frac{1}{2}}\Big),
$$

for $x \in B_{z_j,r}$. Hence

$$
\int_{B_{z_j,r}} (n^2(z_j)-n^2(t))\Phi_\kappa(t,x)G_\kappa(t,z_j)dt = O(r^{1+\alpha}),\ \text{for } x \in B_{z_j,r}.
$$

Since $\nabla H_{\kappa,j}(t,z_j)$ is bounded for $t \in \Omega$, then

$$
\int_{\partial B_{z_j,r}} \partial_{\nu(t)} H_{\kappa,j}(t,z_j)\Phi_{\kappa,j}(t,x)ds(t) = O\Big(\int_{\partial B_{z_j,r}} |\Phi_{\kappa,j}(x,t)|ds(t)\Big) = O(r)
$$

for $x \in \Omega$. Hence, we can write (2.21) as

$$
H_{\kappa,j}(x,z_j) + \int_{\partial B_{z_j,r}} H_{\kappa,j}(t,z_j)\partial_{\nu(t)}\Phi_{\kappa,j}(t,x)ds(t) = O(r),\ \text{for } x \in B_{z_j,r}. \qquad (2.22)
$$

Taking the trace in (2.22) to $\partial B_{z_j,r}$ and using the trace of the double layer potential $\int_{\partial B_{z_j,r}} H_{\kappa,j}(t,z_j)\partial_{\nu(t)}\Phi_{\kappa,j}(t,x)ds(t) = K_r(H_{\kappa,j}(\cdot,z_j))(x) - \frac{1}{2}H_{\kappa,j}(x,z_j),\quad x \in \partial B_{z_j,r}$, where K_r denotes the double layer operator, we derive the equation

$$\left(\frac{1}{2} + K_r\right)(H_{\kappa,j}(\cdot, z_j)) = O(r), \text{ for } x \in \partial B_{z_j,r}. \quad (2.23)$$

Then

$$\|H_{\kappa,j}(\cdot, z_j)\|_{L_2(\partial B_{z_j,r})} = O\left(r \, \|(\frac{1}{2} + K_r)^{-1}\|_{\mathcal{L}(L_2(\partial B_{z_j,r}),\, L_2(\partial B_{z_j,r}))}\right).$$

We have the following estimate from [11]:

$$\|(\frac{1}{2} + K_r)^{-1})\|_{\mathcal{L}(L_2(\partial B_{z_j,r}),\, L_2(\partial B_{z_j,r}))} \leq \|(\frac{1}{2} + K_1)^{-1})\|_{\mathcal{L}(L_2(\partial B),\, L_2(\partial B))}$$

where $B := B_{O,1}$. Hence

$$\|H_{\kappa,j}(\cdot, z_j)\|_{L_2(\partial B_{z_j,r})} = O(r). \quad (2.24)$$

Going back to (2.22), we estimate

$$|H_{\kappa,j}(x, z_j)| \leq \int_{\partial B_{z_j,r}} |H_{\kappa,j}(t, z_j)||\partial_{\nu(t)}\Phi_{\kappa,j}(x, t)|ds(t) + O(r)$$

and then

$$|H_{\kappa,j}(x, z_j)| \leq \|H_{\kappa,j}(\cdot, z_j)\|_{L^2(\partial B_{z_j,r})}\|\|\partial_{\nu(t)}\Phi_{\kappa,j}(\cdot, t)\|_{L^2(\partial B_{z_j,r})} + O(r).$$

From (2.24) and the fact that $\|\partial_{\nu(t)}\Phi_{\kappa,j}(\cdot, t)\|_{L^2(\partial B_{z_j,r})} = O(\int_{\partial B(z_j,r)} |t - z_j|^{-2}dt)^{\frac{1}{2}} = O(1)$, we derive the estimate

$$H_{\kappa,j}(x, z_j) = O(r)$$

for $x \in \overline{B_{z_j,r}}$ and in particular for x such that $|x - z_j| = r$. Hence, from the definition of $H_{\kappa,j}(x, j)$, we deduce that

$$G_\kappa(x, z_j) = \frac{e^{i\kappa n(z_j)|x-z_j|}}{4\pi|x - z_j|} + O(|x - z_j|), \quad \text{as } |x - z_j| \to 0.$$

□

From (2.17), we deduce that,

$$G_\kappa(x, z_j) = \frac{1}{4\pi|x - z_j|} + i\,\kappa\, n(z_j) \; + O(|x - z_j|), \qquad \text{as } |x - z_j| \to 0 \quad (2.25)$$

and then

$$n(z_j) = \lim_{x \to z_j} \left[\frac{1}{i\kappa} G_\kappa(x, z_j) - \frac{1}{i\kappa\; 4\pi|x - z_j|}\right]. \quad (2.26)$$

The formula (2.26) can be used for $x := z_j^2$ and $z_j := z_j^1$, where z_j^1 and z_j^2, $j = 1, 2, ..., M$ are the sampling points added to the small inclusions,

$$n(z_j) = \left[\frac{1}{i\kappa} G_\kappa(z_j^2, z_j^1) - \frac{1}{i\kappa\; 4\pi|z_j^2 - z_j^1|}\right] + O(a^t), \quad t > 0. \quad (2.27)$$

3 Conclusion and comments

We have shown that by deforming a medium with multiple and close inclusions, we can extract the internal values of the coefficients modeling the medium from the far-fields data. We have tested this idea for the acoustic medium modeled by an index of refraction where the small inclusions are impedance type small scatterers.

1. To make this approach fully satisfactory, we need to improve the error in the approximation in (1.8). This is related to the full justification of the Foldy-Lax approximation. The justification of the accuracy and the optimal error estimate in the approximation of the scattered field by the Foldy-Lax field is in its generality a largely open issue but there is an increase of interest to understand it, see for instance [9, 10, 11, 12, 21, 22, 23].

2. Let us consider the more general model $\nabla \cdot c^2 \nabla + \kappa^2 n^2$, where c is the velocity which we assume to be smooth and eventually different from a constant. In this case, arguing as in [13], we can derive the same asymptotic expansion as in (1.8)-(1.9)-(1.10). Hence proceeding as in the three steps we described above, we obtain:
$$\mathbf{C}^{-1}(\mathbf{V}\mathbf{V}^\top)^{-1}\mathbf{V}\left[\mathbf{W}_n^\infty - \mathbf{V}_n^\infty\right]\mathbf{V}^\top(\mathbf{V}\mathbf{V}^\top)^{-1}\mathbf{C}^{-1} + \mathbf{C}^{-1} = \tilde{\mathbf{G}}_\kappa + \quad O\left(a^{1-h-2t} + a^{h-s}\right) \tag{3.1}$$
and instead of (2.17), we obtain
$$G_\kappa(x, z_j) = \left[\frac{e^{i\kappa\frac{n(z_j)}{c(z_j)})|x-z_j|}}{4\pi c^2(z_j)|x - z_j|}\right] + O(\ln(|x - z_j|)), \quad \text{as } |x - z_j| \to 0. \tag{3.2}$$
From (3.2), we derive
$$G_\kappa(x, z_j) = \left[\frac{1}{4\pi c^2(z_j)|x - z_j|}\right] + O(\ln(|x - z_j|)), \quad \text{as } |x - z_j| \to 0. \tag{3.3}$$
Combining (3.3) and (3.1), with $x = z_i^1$ and $z_j := z_i^2$, we derive the formula
$$c^{-2}(z_i) = 4\pi|z_i^1 - z_i^2| \left[\mathbf{C}^{-1}(\mathbf{V}\mathbf{V}^\top)^{-1}\mathbf{V}\left[\mathbf{W}_n^\infty - \mathbf{V}_n^\infty\right]\mathbf{V}^\top(\mathbf{V}\mathbf{V}^\top)^{-1}\mathbf{C}^{-1} + \mathbf{C}^{-1}\right]_{2i-1,2i} \tag{3.4}$$
$$+O(a^t \ln\ a) \quad + O(a^{1-h-2t} + a^{h-s})$$
for $i = 1, ..., M$, recalling that $|z_i^1 - z_i^2| = a^t$, for $i = 1, ..., M$.

We see that we can derive a direct formula linking the measured data $\mathbf{W}_n^\infty$ and $\mathbf{V}_n^\infty$ to the value of the velocity c on sampling points $z_i, i := 1, 2, ..., M$ in Ω. We conclude our discussion with observation that we can push further the asymptotic expansion in (3.2) (or (3.3)) to extract also the values of n at the points $z_i, i := 1, 2, ..., M$.

3. The more realistic model would be $\nabla \cdot c^2 \nabla + \kappa^2 n^2$ where the small perturbations occur in the coefficients c and n and not as small impenetrable obstacles as we dealt with in the present paper. One needs first to derive the corresponding asymptotic expansion taking into account the parameters modeling these small inclusions and then use them to design a reconstruction method to extract c or/and n from similar measured data as we did in the present work. Finally, we do believe that this approach can be applied to other multiwave imaging modalities as well.

Acknowledgement

This work was funded by the Deanship of Scientific Research (DRS), King Abdulaziz University, under the grant no. 20-130-36-HiCi. The authors, therefore, acknowledge with thanks DRS technical and financial support.

References

[1] G. Alessandrini. Global stability for a coupled physics inverse problem. *Inverse Problems* 30 (2014), no. 7, 075008, 10 pp.

[2] G. S. Alberti. On multiple frequency power density measurements. *Inverse Problems* 29 (2013), no. 11, 115007, 25 pp.

[3] H. Ammari; E. Bonnetier; Y. Capdeboscq; M. Tanter; M. Fink. Electrical impedance tomography by elastic deformation. *SIAM J. Appl. Math.* 68 (2008), no. 6, 1557-1573.

[4] H. Ammari. An introduction to mathematics of emerging biomedical imaging. Mathematics and Applications, 62. Springer, Berlin, 2008.

[5] H. Ammari; Y. Capdeboscq; F. de Gournay; A. Rozanova-Pierrat; F. Triki. Microwave imaging by elastic deformation. *SIAM J. Appl. Math.* 71 (2011), no. 6, 2112-2130.

[6] H. Ammari; J. Garnier; W. Jing. Resolution and stability analysis in acousto-electric imaging. Inverse Problems 28 (2012), no. 8, 084005, 20 pp.

[7] G. Bal; E. Bonnetier; F. Monard; F. Triki. Inverse diffusion from knowledge of power densities. *Inverse Probl. Imaging* 7 (2013), no. 2, 353375.

[8] G. Bal. Hybrid inverse problems and redundant systems of partial differential equations. *Inverse problems and applications,* 1547, Contemp. Math., 615, Amer. Math. Soc., Providence, RI, 2014.

[9] A. Bendali, P.-H. Cocquet, and S. Tordeux. Scattering of a scalar time-harmonic wave by n small spheres by the method of matched asymptotic expansions. *Numerical Analysis and Applications*, 5(2):116–123, 2012.

[10] M. Cassier and C. Hazard. Multiple scattering of acoustic waves by small sound-soft obstacles in two dimensions: mathematical justification of the Foldy-Lax model. *Wave Motion*, 50(1):18–28, 2013.

[11] D. P. Challa and M. Sini. On the justification of the Foldy-Lax approximation for the acoustic scattering by small rigid bodies of arbitrary shapes. *Multiscale Model. Simul.*, 12(1):55–108, 2014.

[12] D. P. Challa; M. Sini. The Foldy-Lax approximation of the scattered waves by many small bodies for the Lame system. Mathematische Nachrischten, to appear, `arXiv: 1308.3072`.

[13] D. P. Challa; M. Sini. Multiscale analysis of the acoustic scattering by many scatterers of impedance type. Preprint, `arXiv:1504.02665`.

[14] D. L. Colton and R. Kress. *Integral equation methods in scattering theory*. Pure and Applied Mathematics (New York). John Wiley & Sons Inc., New York, 1983. A Wiley-Interscience Publication.

[15] D. Colton and R. Kress. *Inverse acoustic and electromagnetic scattering theory*, volume 93 of *Applied Mathematical Sciences*. Springer-Verlag, Berlin, second edition, 1998.

[16] M. Fink and M. Tanter. Multiwave imaging and super resolution. *Physics Today* 63, no. 2 (2010): 28-33.

[17] M. Fink and M. Tanter. A multiwave imaging approach for elastography. *Current Medical Imaging Reviews* 7, no. 4 (2011): 340-349.

[18] N. Honda; J. McLaughlin; G. Nakamura. Conditional stability for a single interior measurement. *Inverse Problems* 30 (2014), no. 5, 055001,

[19] A. Kirsch and N. Grinberg. *The factorization method for inverse problems*, volume 36 of *Oxford Lecture Series in Mathematics and its Applications*. Oxford University Press, Oxford, 2008.

[20] G. Lerosey and M. Fink. Acousto-optic imaging: Merging the best of two worlds. *Nature Photonics* 7, no. 4 (2013): 265267

[21] V. Mazýa and A. Movchan. Asymptotic treatment of perforated domains without homogenization. *Math. Nachr.*, 283(1):104–125, 2010.

[22] V. Mazýa, A. Movchan, and M. Nieves. Mesoscale asymptotic approximations to solutions of mixed boundary value problems in perforated domains. *Multiscale Model. Simul.*, 9(1):424–448, 2011.

[23] V. Maz'ya, A. Movchan, and M. Nieves. *Green's kernels and meso-scale approximations in perforated domains*, volume 2077 of *Lecture Notes in Mathematics*. Springer, Heidelberg, 2013.

[24] W. McLean. *Strongly elliptic systems and boundary integral equations*. Cambridge University Press, Cambridge, 2000.

[25] A. I. Nachman. Reconstructions from boundary measurements. Ann. of Math. (2) 128 (1988), no. 3, 53176.

[26] R. G. Novikov. A multidimensional inverse spectral problem for the equation $\Delta\psi + (v(x) - Eu(x))\psi = 0$. Funct. Anal. Appl. 22 (1988), no. 4, 26372.

[27] A. G. Ramm. Recovery of the potential from fixed-energy scattering data. Inverse Problems 4 (1988), no. 3, 87786.

[28] A. G. Ramm. *Wave scattering by small bodies of arbitrary shapes*. World Scientific Publishing Co. Pte. Ltd., Hackensack, NJ, 2005.

[29] F. Triki. Uniqueness and stability for the inverse medium problem with internal data. *Inverse Problems* 26 (2010), no. 9, 095014,

[30] N. Valdivia. Uniqueness in inverse obstacle scattering with conductive boundary conditions. *Appl. Anal.* 83 (2004), no. 8, 825-851.